

SYNTHESIS AND PROPERTIES OF INORGANIC COMPOUNDS

Synthesis and Structure of Alkali Metal Zirconium Vanadate Phosphates

V. I. Pet'kov^a, M. V. Sukhanov^a, A. S. Shipilov^a, V. S. Kurazhkovskaya^b, E. Yu. Borovikova^b,
N. V. Sakharov^a, M. M. Ermilova^c, and N. V. Orekhova^c

^a Lobachevsky State University of Nizhni Novgorod, pr. Gagarina 23, Nizhni Novgorod, 603950 Russia

^b Moscow State University, Vorob'evy gory, Moscow, 119899 Russia

^c Topchiev Institute of Petrochemical Synthesis, Russian Academy of Sciences, Leninskii pr. 29, Moscow, 119991 Russia

Received September 5, 2012

Abstract—Mixed vanadate phosphates in the systems $MZr_2(VO_4)_x(PO_4)_{3-x}$, where M is an alkali metal, were synthesized and studied by X-ray diffraction, electron probe microanalysis, and IR spectroscopy. Substitutional solid solutions with the structure of the mineral kosnarite (NKP) are formed at the compositions $0 \leq x \leq 0.2$ for M = Li; $0 \leq x \leq 0.4$ for M = Na; $0 \leq x \leq 0.5$ for M = K; $0 \leq x \leq 0.3$ for M = Rb; and $0 \leq x \leq 0.2$ for M = Cs. Apart from the high-temperature NKP modification, lithium vanadate phosphates $LiZr_2(VO_4)_x(PO_4)_{3-x}$ with $0 \leq x \leq 0.8$ synthesized at temperatures not exceeding 840°C crystallize in the scandium tungstate type structure. The crystal structures of $LiZr_2(VO_4)_{0.8}(PO_4)_{2.2}$ (space group $P2_1/n$, $a = 8.8447(6)$ Å, $b = 8.9876(7)$ Å, $c = 12.3976(7)$ Å, $\beta = 90.821(4)^\circ$, $V = 985.4(1)$ Å³, $Z = 4$) and $NaZr_2(VO_4)_{0.4}(PO_4)_{2.6}$ (space group $R\bar{3}c$, $a = 8.8182(3)$ Å, $c = 22.7814(6)$ Å, $V = 1534.14(1)$ Å³, $Z = 6$) were refined by the Rietveld method. The framework of the vanadate phosphate structure is composed of tetrahedra (that are statistically occupied by vanadium and phosphorus atoms) and ZrO_6 octahedra. The alkali metal atoms occupy extra-framework sites.

DOI: 10.1134/S0036023613090167

The family of the mineral kosnarite $KZr_2(PO_4)_3$, which is often called NKP after the first synthesized isoformula analog $NaZr_2(PO_4)_3$ (space group $R\bar{3}c$, $a = 8.8045(3)$ Å, $c = 22.7581(7)$ Å) [1], is a classical object of investigation of isomorphism owing to its pronounced tendency of ion substitution in any of crystallographic sites with retention of the structural motif. The possibility of using structural information about the size and the number of occupied polyhedra for targeted change in the phase composition can ensure the maximum utility of the designed material [2]. It is of interest to use representatives of the NKP family as solid electrolytes, ceramics with low thermal expansion, materials for incorporating radioactive wastes, catalysts, and biomaterials compatible with bone tissue [2, 3]. The iso- and heterovalent substitution in Na and Zr sites of synthetic NKP compounds often gives rise to solid solutions. The substitutions in phosphorus sites are still little studied. Exceptions are silicophosphates $Na_{1+x}Zr_2Si_xP_{3-x}O_{12}$ (NASICON), owing to their high cationic conductivity [4]. Depending on the composition of silicophosphates, the unit cell symmetry varies from trigonal to monoclinic with retention of the overall NKP architecture. Vanadium-containing solid solutions $Li_{1.3}Al_{0.3}Ti_{1.7}(VO_4)_x(PO_4)_{3-x}$ ($x \leq 0.1$), the vanadate $Ag_3Sc_2(VO_4)_3$, and mixed vanadate phosphates based on it, which crystallize in an NKP type

structure, are known [5, 6]. We showed that the replacement of phosphorus by arsenic affords a continuous series of solid solutions $NaZr_2(AsO_4)_x(PO_4)_{3-x}$ with the NKP structure [7], while the replacement of phosphorus by molybdenum yields limited solid solutions $M_{1-x}Zr_2(MoO_4)_x(PO_4)_{3-x}$ (M = Na, K, Rb, Cs) [8, 9]. The crystallization field of the molybdate phosphates with the NKP structure is contracted as the size of the alkali metal cation increases.

The understanding of factors affecting the patterns and the degree of anionic substitution within a particular structural type would allow prediction of the structure and properties of the resulting phases of variable composition. Owing to the acidic nature of V_2O_5 and P_2O_5 and relatively small difference between the V–O and P–O bond lengths in the VO_4 and PO_4 tetrahedra (~12%) with considerable difference between the electronegativities ($\Delta = 0.56$), one can expect restricted isomorphism in the predicted series of vanadate phosphates $MZr_2(VO_4)_x(PO_4)_{3-x}$ with alkali metals (M).

This work deals with replacement of phosphorus by vanadium in the systems $MZr_2(VO_4)_x(PO_4)_{3-x}$ (M = Li, Na, K, Rb, Cs) and effect of crystal chemical characteristics of alkali metals on the limits of $P^{5+} \leftrightarrow V^{5+}$ isomorphous substitution and structurization of solid solutions.

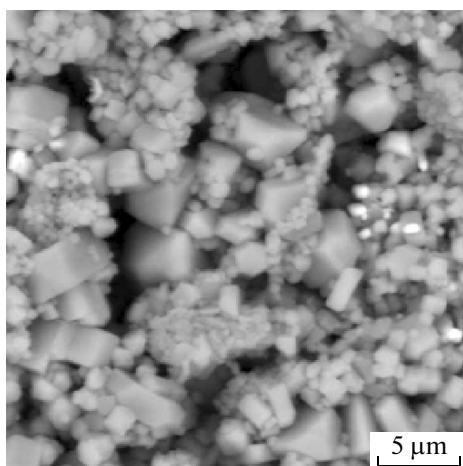


Fig. 1. Electron microscopic image of the vanadate phosphate $\text{LiZr}_2(\text{VO}_4)_{0.2}(\text{PO}_4)_{2.8}$ (grains that are brighter than the major material are zirconium oxide).

EXPERIMENTAL

It was planned to prepare vanadate phosphates $\text{MZr}_2(\text{VO}_4)_x(\text{PO}_4)_{3-x}$ with $\text{M} = \text{Li}, \text{Na}, \text{K}, \text{Rb}, \text{Cs}$ in the range of x from 0 to 3. The synthesis was performed by precipitation from solutions of alkali metal nitrates, zirconium oxychloride, phosphoric acid, and ammonium metavanadate. Reagent grade chemicals were used. The reaction mixtures were dried at 90°C and heat-treated with free access of air in porcelain or platinum crucibles at 200, 600, 800–850, and 950°C for at least 24 h in each stage. The samples were synthesized using the ZnO sintering additive (0.75 wt %), which promotes tighter contact of powder grains, increases the rates of solid-state reactions, and decreases the synthesis temperature [10]. Zinc oxide was added to samples annealed at 600°C and then pellets were pressed at 200 MPa and annealed at 800–850°C. The stepwise heating alternated with dispersing. The resulting samples were yellow-brown polycrystalline powders.

Table 1. Unit cell parameters of vanadate phosphates $\text{MZr}_2(\text{VO}_4)_x(\text{PO}_4)_{3-x}$ ($\text{M} = \text{Li}, \text{Na}, \text{K}, \text{Rb}, \text{Cs}$)

M	x	The unit cell parameters		
		$a, \text{\AA}$	$c, \text{\AA}$	$V, \text{\AA}^3$
Li	0.2	8.875(1)	22.265(3)	1518.6(4)
Na	0.4	8.827(2)	22.799(9)	1538.4(5)
K	0.5	8.733(3)	23.96(2)	1583(2)
Rb	0.3	8.678(1)	24.402(8)	1592(1)
Cs	0.2	8.595(2)	24.990(9)	1598.8(6)

The chemical composition and homogeneity of the final products were examined using a Jeol JSM-6490 scanning electron microscope equipped with secondary and reflected electron detector and an INCA 350 energy-dispersive X-ray microanalyzer. The error of determination of the composition of samples was not more than 2 at %. Analysis of the obtained images of the structure leads to the conclusion that the grain structure of the samples is inhomogeneous, and the grain size varies from 1 to 10 μm . Microprobe analysis data of single-phase samples showed a homogeneous composition of grains and the correspondence to the theoretical x value with allowance for the error of the method. In some photomicrographs (Fig. 1), one can see ZrO_2 grains that are brighter than the major material; this attests to substitution of Zn for minor amounts of Zr in the vanadate phosphate structure due to the use of ZnO additive.

The X-ray diffraction patterns of the samples were measured on an XRD-6000 diffractometer ($\text{CuK}\alpha$ radiation, $\lambda = 1.54178 \text{ \AA}$, 2θ range 10° – 50°). The X-ray diffraction spectra for refinement of the structure of the vanadate phosphates $\text{LiZr}_2(\text{VO}_4)_{0.8}(\text{PO}_4)_{2.2}$ and $\text{NaZr}_2(\text{VO}_4)_{0.4}(\text{PO}_4)_{2.6}$ were measured in the 2θ range from 10° to 110° with a step of 0.02° and a 2.5 s exposure at each point. The structure was refined by the Rietveld method [11] using the RIETAN-97 program package [12]. The peak profiles were approximated by the modified pseudo-Voigt function (ModTCH pV [13]). The atom coordinates of $\text{LiZr}_2(\text{PO}_4)_3$ [14] and $\text{NaZr}_2(\text{PO}_4)_3$ [1] were used as the basic models for crystal structure refinement of vanadate phosphates.

The functional composition of samples was confirmed by IR spectroscopic measurements. The absorption spectra were recorded on a FSM-1201 IR spectrometer in the 400 – 1400 cm^{-1} range of wavelengths.

RESULTS AND DISCUSSION

The results of powder X-ray diffraction indicate that at the synthesis temperature of 600°C , the samples $\text{MZr}_2\text{V}_x\text{P}_{3-x}\text{O}_{12}$ ($\text{M} = \text{Na}, \text{K}, \text{Rb}, \text{Cs}$) with $x < 3$ are mixtures of crystalline phases: NZP phase, and ZrO_2 ; the samples with $x = 3$ are amorphous to X-rays. The use of the sintering additive ZnO at 850°C gave single-phase samples of $\text{MZr}_2(\text{VO}_4)_x(\text{PO}_4)_{3-x}$ with an NZP type structure in the range of $0 \leq x \leq 0.4$ for $\text{M} = \text{Na}$, $0 \leq x \leq 0.5$ for $\text{M} = \text{K}$, $0 \leq x \leq 0.3$ for $\text{M} = \text{Rb}$, $0 \leq x \leq 0.2$ for $\text{M} = \text{Cs}$. The unit cell parameters of the single-phase samples in the series $\text{MZr}_2(\text{VO}_4)_x(\text{PO}_4)_{3-x}$ with the M^+ cation being the same smoothly increase with an increase in the content of V^{5+} ($r_{\text{CN}4} = 0.355 \text{ \AA}$), which is larger than P^{5+} ($r_{\text{CN}4} = 0.17 \text{ \AA}$). The unit cell parameters of the terminal members of solid solutions of vanadate phosphates are given in Table 1; as the radius of the alkali metal cation or the V : P ratio increases, regular increase in the parameter c and

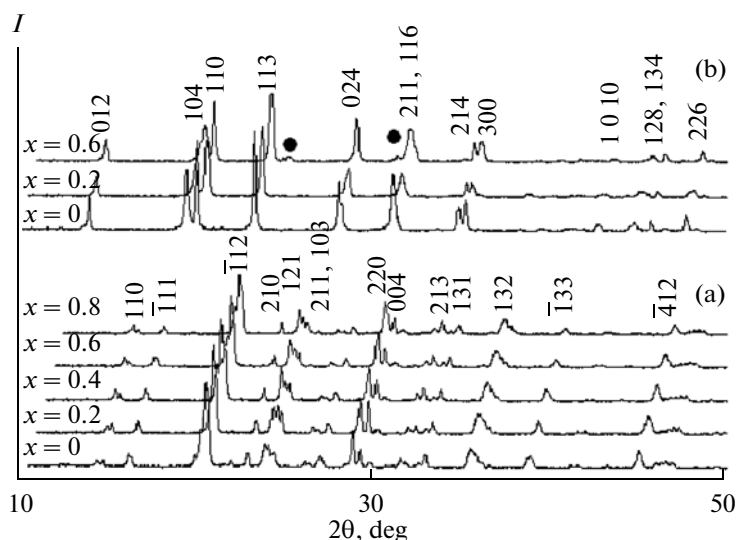


Fig. 2. X-ray diffraction patterns of samples of $\text{LiZr}_2(\text{VO}_4)_x(\text{PO}_4)_{3-x}$ with different degrees of substitution ($x = 0, 0.2, 0.4, 0.6$, and 0.8) synthesized at (a) $800\text{--}840^\circ\text{C}$ and (b) 850°C and crystallizing in the (a) SW and (b) NZP structural type.

decrease in the parameter a take place. This is due to the fact that in the NZP type framework structure, the M^+ cation is located within infinite columns of the ZrO_6 octahedra and $(\text{P,V})\text{O}_4$ tetrahedra, which are combined through common oxygen atoms and are parallel to axis 3 (axis c of the unit cell). When larger M^+ cations are inserted into the cavities, this makes a larger contribution to the increase in the parameter c of vanadate phosphates as compared with the slight increase in the bond lengths and bond angles of the PO_4 tetrahedra caused by low content of vanadium in them. The deformation of the $(\text{P,V})\text{O}_4$ tetrahedra caused by insertion of larger-size M^+ cations into the cavities within the columns leads to increase in the $\text{O}-(\text{P,V})-\text{O}$ internal angle along the c axis, which reduces the distance between the parallel columns and thus decreases the parameter a .

The increase in the annealing temperature of solid solutions to 950°C resulted, according to powder X-ray diffraction data, in appearance of zirconium oxide impurity, shift of reflections of the target phases to greater angles, and decrease in the unit cell parameters of these phases, indicating that the vanadium content in the solid solutions decreases.

A more complicated phase formation pattern was observed in $\text{LiZr}_2(\text{VO}_4)_x(\text{PO}_4)_{3-x}$. The annealing of these samples at $800\text{--}840^\circ\text{C}$ induced crystallization of the phases $\text{Sc}_2(\text{WO}_4)_3$ (SW) in the range of $0 \leq x \leq 0.8$ (Fig. 2). The unit cell parameters of single-phase samples increase with increase in the vanadium content in the series of $\text{LiZr}_2(\text{VO}_4)_x(\text{PO}_4)_{3-x}$ (Fig. 3). Powder X-ray diffraction of samples with $x \geq 1.0$ showed that they were not single phases; the major phase was of the NZP structural type and had similar unit cell parameters. The microprobe analysis indicates that the composition of the NZP phase is $\text{LiZr}_2(\text{VO}_4)_{0.2}(\text{PO}_4)_{2.8}$. An

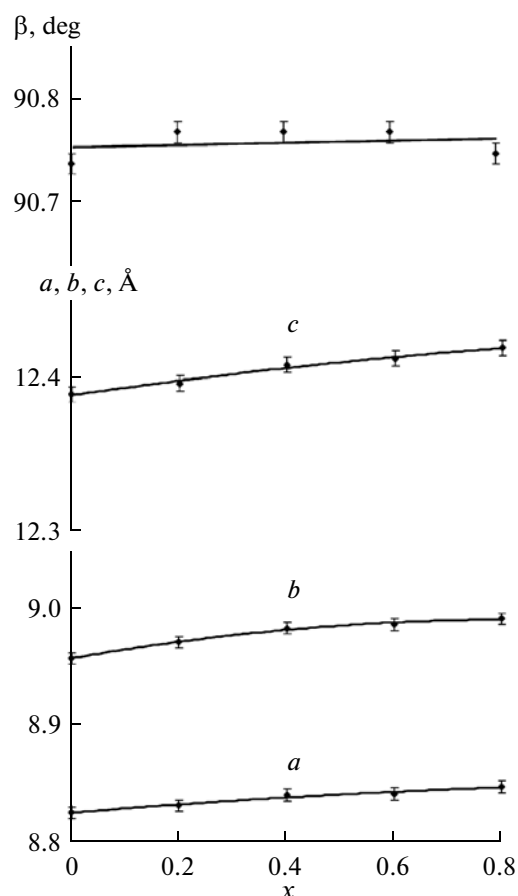


Fig. 3. Unit cell parameters of the vanadate phosphates $\text{LiZr}_2(\text{VO}_4)_x(\text{PO}_4)_{3-x}$ crystallizing in the scandium tungstate structural type vs. composition.

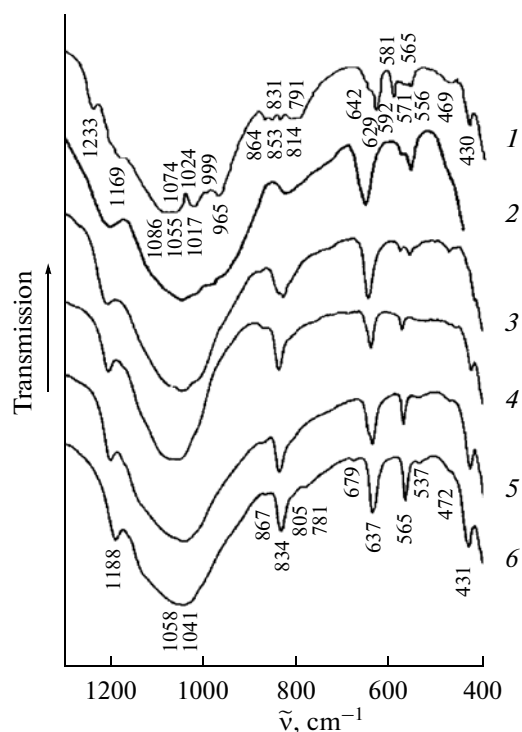


Fig. 4. IR spectra of $MZr_2(VO_4)_x(PO_4)_{3-x}$: (1) $M = Li$, $x = 0.4$; (2) $M = Li$, $x = 0.2$; $M = Na$, $x = 0.4$; (3) $M = K$, $x = 0.5$; (4) $M = Rb$, $x = 0.3$; (5) $M = Cs$, $x = 0.2$.

increase in the annealing temperature to 850°C gave rise to NZP phase reflections in the X-ray diffraction patterns of $LiZr_2V_xP_{3-x}O_{12}$ with $0 \leq x \leq 0.2$. For the composition of $0.2 < x \leq 0.8$, an NZP phase with the composition $LiZr_2(VO_4)_{0.2}(PO_4)_{2.8}$ and a zirconium oxide impurity were formed.

Crystallization in the NZP and SW structural types is known for the phosphate $LiZr_2(PO_4)_3$ ($x = 0$). The $LiZr_2(PO_4)_3$ sample synthesized at 1200°C has a rhombohedral unit cell symmetry (space group $R\bar{3}c$) at a temperature of >50°C [15]. If the phosphate synthesis is carried out at a temperature not exceeding 900°C, the compound crystallizes in the monoclinic modification of the $Sc_2(WO_4)_3$ structural type (space group $P2_1/n$) [14]. An increase in the vanadium content in $LiZr_2(VO_4)_x(PO_4)_{3-x}$ reduces the temperature of the phase transition SW (space group $P2_1/n$) → NZP (space group $R\bar{3}c$). The concentration field of the existence of the NZP structure in the $LiZr_2(VO_4)_x(PO_4)_{3-x}$ system is narrower than that of the scandium tungstate structure. This may be due to the fact that the NZP structure has one type of sites for the anion-forming phosphorus and vanadium ions, while in the structure of monoclinic scandium tungstate, there are three types of such sites. Differentiation of the sites of anion-forming atoms (and, hence, the bond lengths and bond angles) gives rise to a

greater stability region of the VO_4^{3-} tetrahedra in combination with smaller tetrahedral phosphorus cations.

No single-phase samples with $x = 3$ were formed at any annealing temperature. Crystallization of these mixtures in a porcelain crucible (made of aluminosilicate ceramics) at 1000–1270°C gave rise to X-ray reflections intrinsic in compounds with the zircon structure. In this temperature range, the reaction mixtures reacted with the crucible material to give the zircon phase $Zr_{1.03(1)}V_{0.06(2)}Si_{0.86(2)}O_4$; low vanadium content in the sample is due to sublimation of vanadium oxide. When a platinum crucible is used, a phase with the zircon structure and the presumptive composition $ZrV^{4+}O_4$ and ZrO_2 is formed.

Analysis of the IR spectra of the single-phase vanadate phosphate samples indicated the presence of the PO_4 and VO_4 groups and the absence of condensed phosphates and vanadates. Figure 4 shows the IR spectra of alkali metal zirconium vanadate phosphates, which crystallize in two space groups, $P2_1/n$ and $R\bar{3}c$. The number of observed bands in the IR spectrum of $LiZr_2(VO_4)_{0.4}(PO_4)_{2.6}$ is much less than that predicted by the selection rules but is still rather great (Fig. 4, spectrum 1). According to the selection rules, the IR spectra of mixed lithium zirconium vanadate phosphates (space group $P2_1/n$) may exhibit 18 asymmetric stretching bands ν_3 and 6 symmetric stretching bands ν_1 . The bands at 1233–1017 cm^{-1} can be assigned to the asymmetric stretching modes ν_3 , while two bands at 999 and 965 cm^{-1} can be assigned to the symmetric stretching modes ν_1 of the PO_4^{3-} ions. The 642–556 cm^{-1} region displays 7 out of the 18 asymmetric bending modes ν_4 allowed by the selection rules. The 469 and 430 cm^{-1} bands correspond to symmetric bending modes ν_2 . Five out of the 18 possible weak bands in the central part of the spectrum (870–790 cm^{-1}) correspond to the VO_4^{3-} stretching vibrations.

The other vanadate phosphates the spectra of which are shown in Fig. 4 have space group $R\bar{3}c$. According to selection rules, the IR spectra may exhibit five asymmetric stretching bands ν_3 , one symmetric stretching band ν_1 , five asymmetric bending bands ν_4 , and two symmetric bending bands ν_2 . The number of bands in all regions of the spectra of NZP type vanadate phosphates decreases as compared with the spectrum of the monoclinic phase. In the phosphate stretching region, one broad band is present with a maximum at ~1040 cm^{-1} in which five bands predicted by the selection rules overlap. At 680–530 cm^{-1} , two to four bending bands are present, while in the vanadate ion region (880–780 cm^{-1}), one medium-intensity band occurs at ~840 cm^{-1} being accompanied by several shoulders. The spectral pattern of the

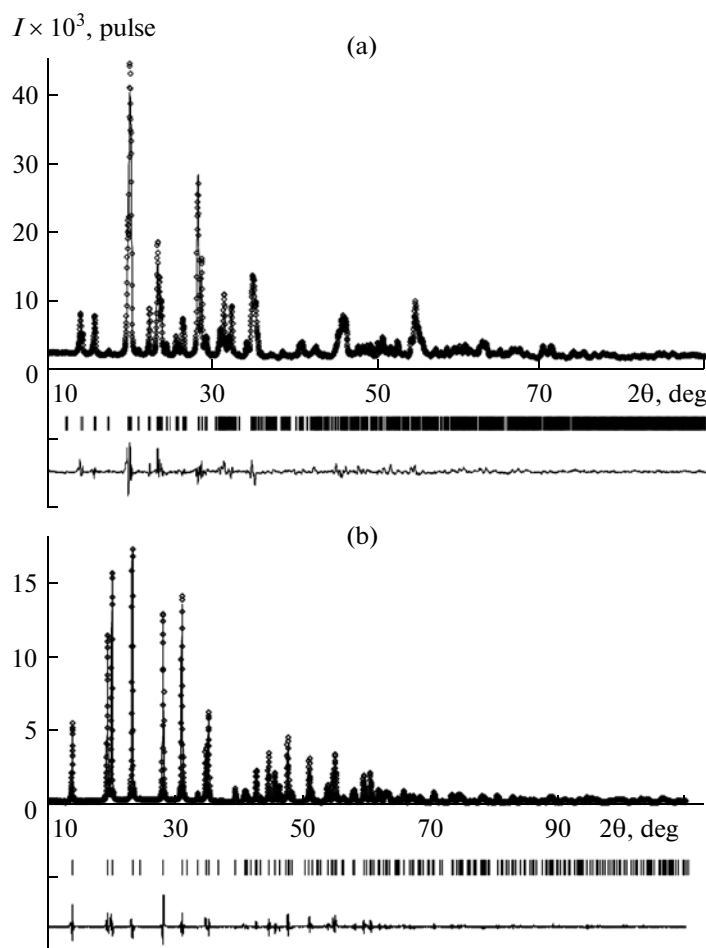


Fig. 5. Experimental (circles) and simulated (continuous line) X-ray diffraction spectra of (a) $\text{LiZr}_2(\text{VO}_4)_{0.8}(\text{PO}_4)_{2.2}$ and (b) $\text{NaZr}_2(\text{VO}_4)_{0.4}(\text{PO}_4)_{2.6}$. The vertical strokes show the positions of reflections of the theoretical X-ray diffraction pattern; the curve in the bottom is the difference intensity curve of the experimental and theoretical spectra.

VO_4^{3-} ion modes is similar to that observed for PO_4^{3-} stretching modes.

Thus, the IR spectra of vanadate phosphates present in Fig. 4 have both common and distinct features depending on the space group (monoclinic or orthorhombic) in which the given phase crystallizes. Vanadium is present in the phosphate structures and occupies the same positions as phosphorus, as indicated by the form and the number of bands for the VO_4^{3-} ion.

The crystal structures of $\text{LiZr}_2(\text{VO}_4)_{0.8}(\text{PO}_4)_{2.2}$ and $\text{NaZr}_2(\text{VO}_4)_{0.4}(\text{PO}_4)_{2.6}$ were refined based on powder X-ray diffraction data by the Rietveld method (Fig. 5). The data collection details, the unit cell parameters, and structure refinement parameters are summarized in Table 2. The atom coordinates and isotropic thermal parameters and cationic site occupancies are given in Tables 3 and 4. The structures of vanadate phosphates are depicted in Fig. 6.

The crystal structure of the vanadate phosphate $\text{LiZr}_2(\text{VO}_4)_{0.8}(\text{PO}_4)_{2.2}$ was refined in the space group $P2_1/n$. The obtained data indicate that the crystal structure corresponds to the SW type. The isolated ZrO_6 octahedra and $(\text{P,V})\text{O}_4$ tetrahedra form a three-dimensional framework by sharing vertices. The Zr–O bond lengths are typical of six-coordinate zirconium, the average Zr–O distances in the coordination polyhedra being somewhat non-equivalent (2.06 and 2.15 Å). The ratio of bond lengths and bond angles in the $(\text{P,V})\text{O}_4$ tetrahedra is usual. The average (P,V) –O bond lengths in the $(\text{P,V})\text{O}_4$ polyhedra vary from 1.53 to 1.67 Å. Two ZrO_6 octahedra and three tetrahedra statistically occupied by vanadium and phosphorus atoms (and the small cavity shaped like a trigonal prism between the octahedra) form a topological unit of the framework, a “lantern” (Fig. 6a). These structural units are packed in zigzag-like ribbons. Neighboring lanterns in the same ribbon form an acute angle of 71° , and a herring-bone packing of the structural units is formed. The framework cavities have a complex shape and a relatively small volume. Lithium atoms

Table 2. Data collection details, unit cell parameters and selected structure refinement data for $\text{LiZr}_2(\text{VO}_4)_{0.8}(\text{PO}_4)_{2.2}$ and $\text{NaZr}_2(\text{VO}_4)_{0.4}(\text{PO}_4)_{2.6}$

Compound	$\text{LiZr}_2(\text{VO}_4)_{0.8}(\text{PO}_4)_{2.2}$	$\text{NaZr}_2(\text{VO}_4)_{0.4}(\text{PO}_4)_{2.6}$
Space group	$P2_1/n$	$R\bar{3}c$
Z	4	6
Angle range, 2θ , deg	10–90	10–110
Unit cell parameters:		
a , Å	8.8447(6)	8.8182(3)
b , Å	8.9876(7)	22.7814(6)
c , Å	12.3976(7)	—
β , deg	90.821(4)	90
V , Å ³	985.4(1)	1534.14(8)
The number of reflections	987	291
The number of refined parameters:		
structural	56	15
other	22	18
R -factors		
R_{wp} , R_{p}	7.58, 5.83	8.30, 5.82

Table 3. Atom coordinates and isotropic thermal parameters of $\text{LiZr}_2(\text{VO}_4)_{0.8}(\text{PO}_4)_{2.2}$

Atom	x	y	z	B , Å ²
Li	0.2904(1)	0.2186(0)	0.3279(8)	3.2(1)
Zr(1)	0.7578(9)	0.4556(8)	0.6178(7)	3.2(1)
Zr(2)	0.7654(9)	0.0230(8)	0.3823(7)	3.2(1)
(P,V)(1)	0.605(3)	0.106(2)	0.619(2)	3.2(1)
(P,V)(2)	0.615(2)	0.372(2)	0.358(2)	3.2(1)
(P,V)(3)	0.039(2)	0.272(2)	0.499(2)	3.2(1)
O(1)	0.676(6)	0.422(4)	0.459(4)	3.2(1)
O(2)	0.684(5)	0.237(4)	0.658(4)	3.2(1)
O(3)	0.937(5)	0.371(5)	0.564(4)	3.2(1)
O(4)	0.568(4)	0.5605(4)	0.669(4)	3.2(1)
O(5)	0.844(5)	0.463(5)	0.778(3)	3.2(1)
O(6)	0.849(6)	0.661(5)	0.601(4)	3.2(1)
O(7)	0.673(4)	0.034(5)	0.539(4)	3.2(1)
O(8)	0.638(5)	0.199(5)	0.306(4)	3.2(1)
O(9)	0.911(5)	0.214(4)	0.402(4)	3.2(1)
O(10)	0.544(6)	0.892(4)	0.343(4)	3.2(1)
O(11)	0.776(5)	−0.007(5)	0.207(4)	3.2(1)
O(12)	0.845(5)	0.845(5)	0.423(4)	3.2(1)

Note: P, V site occupancy: $[0.73\text{P}^{5+} + 0.27\text{V}^{5+}]$. Positions of all atoms 4e.

Table 4. Atom coordinates and isotropic thermal parameters of $\text{NaZr}_2(\text{VO}_4)_{0.4}(\text{PO}_4)_{2.6}$

Atom	Site	x	y	z	B , Å ²
Na	6b	0	0	0	3.0(2)
Zr	12c	0	0	0.1452(1)	0.56(5)
(P,V)	18e	0.2870(1)	0	0.25	2.1(1)
O(1)	36f	0.1789(6)	−0.0316(8)	0.1942(3)	1.6(2)
O(2)	36f	0.1873(6)	0.1625(6)	0.0858(2)	1.3(2)

(CN 4) occur in the narrow area of the cavities between the edges of two zirconium octahedra (Fig. 6a). The Li–O distances are in the range of 1.86–2.34 Å.

The vanadate phosphate $\text{NaZr}_2(\text{VO}_4)_{0.4}(\text{PO}_4)_{2.6}$ crystallizes in the NZP type with the space group $R\bar{3}c$. Its crystal structure is formed by a framework of nearly regular ZrO_6 octahedra combined by sharing oxygen atoms (Zr–O , 2.06 Å) and distorted (P,V) O_4 tetrahedra in which the (P,V) atoms are surrounded by two pairs of equally distant oxygen atoms ((P,V)–O, 1.53–1.61 Å). The lanterns form infinite columns parallel to axis 3 and produce a stack packing of structural units (Fig. 6b). The octahedral cavities of the framework present between the lanterns inside the columns are fully occupied by sodium cations (Na occurs at the midpoint of a nearly regular octahedron with an average Na–O distance of 2.50 Å), while the cavities between the neighboring columns remain vacant (Fig. 6b).

The number and the shape of cavities arising in the framework are the most important consequences of different spatial arrangements of Zr and (P,V) polyhedra in the monoclinic and rhombohedral frameworks. In both cases, the same structural units, lanterns (packed in different modes), and the general architecture of the structure are retained. The miscibility of anions in the $\text{MZr}_2(\text{VO}_4)_x(\text{PO}_4)_{3-x}$ systems depends not only on the ratio of the V–O and P–O bond lengths but also on the alkali metal cation size. The size of potassium is the best for the highest anion miscibility in the NZP structure to be achieved. A larger or smaller alkali metal cations narrow down the miscibility region due to structure deformation. The most pronounced deformation occurs for the lithium system: the synthesis of samples at a temperature not exceeding 840°C results in the crystallization of phases with a scandium tungstate type structure.

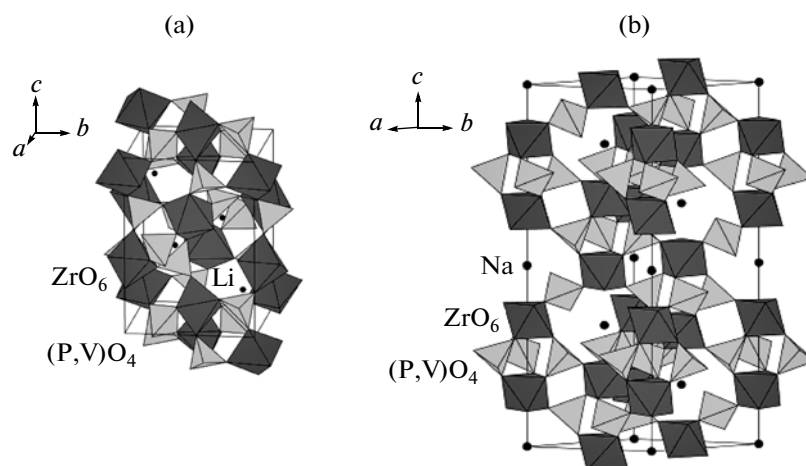


Fig. 6. Structure of the vanadate phosphates (a) $\text{LiZr}_2(\text{VO}_4)_{0.8}(\text{PO}_4)_{2.2}$ and (b) $\text{NaZr}_2(\text{VO}_4)_{0.4}(\text{PO}_4)_{2.6}$.

ACKNOWLEDGMENTS

This work was supported by the Russian Foundation for Basic Research (project no. 11-03-00082).

REFERENCES

1. L. Hagman and P. Kierkegaard, *Acta Chem. Scand.* **22**, 1822 (1968).
2. V. I. Pet'kov, *Russ. Chem. Rev.* **81**, 606 (2012).
3. V. I. Pet'kov and A. I. Orlova, *Inorg. Mater.* **39**, 1013 (2003).
4. A. K. Ivanov-Shits and I. V. Murin, *Solid State Ionics* (Izd. SPbGU, St. Petersburg, 2001), Vol. 1 [in Russian].
5. A. S. Best and P. J. Newman, D. R. MacFarlane, et al., *Solid State Ionics* **126**, 191 (1999).
6. O. I. Solovyov and L. N. Komissarova, *Book of Abstracts, 10th Conference on Solid State Chemistry, Univ. of Pardubice, 2012*, p. 106.
7. M. V. Sukhanov, V. I. Pet'kov, D. V. Firsov, et al., *Russ. J. Inorg. Chem.* **56**, 1351 (2011).
8. V. I. Pet'kov, M. V. Sukhanov, and V. S. Kurazhkovskaya, *Radiochemistry* **45**, 620 (2003).
9. M. V. Sukhanov, V. I. Pet'kov, V. S. Kurazhkovskaya, et al., *Russ. J. Inorg. Chem.* **51**, 706 (2006).
10. M. V. Sukhanov, V. I. Pet'kov, and D. V. Firsov, *Inorg. Mater.* **47**, 674 (2011).
11. H. M. Rietveld, *Acta Crystallogr.* **22**, 151 (1967).
12. Y. I. Kim and F. Izumi, *J. Ceram. Soc. Jpn.* **102**, 401 (1994).
13. F. Izumi, *The Rietveld Method*, Ed. by R. A. Ch. Young (Oxford Univ. Press, New York, 1993).
14. M. Catti, N. Morgante, and R. M. Ibberson, *J. Solid State Chem.* **152**, 340 (2000).
15. M. Catti and S. Stramare, *Solid State Ionics* **136–137**, 489 (1999).

Translated by Z. Svitanko